https://doi.org/10.5194/acp-2019-957
Preprint. Discussion started: 10 December 2019

Atmospheric Chemistry and Physics Discussions

Biomass burning induced surface darkening and its impact on regional meteorology in eastern China

Rong Tang[1,2], Xin Huang[1,2,*], Derong Zhou[1,2], and Aijun Ding[1,2]

[1]School of Atmospheric Sciences, Nanjing University, Nanjing, 210023, China
[2]Collaborative Innovation Center of Climate Change, Jiangsu Province, Nanjing, 210023, China

Correspondence to: Xin Huang (xinhuang@nju.edu.cn)

Abstract. Biomass burning has attracted great concerns for the emission of particular matters and trace gases, which substantially impact air quality, human health and climate change. Meanwhile, large areas of dark char, carbon residue produced in incomplete combustion, can stick to the surface over fire prone areas after open burning, leading to a sharp drop in surface albedo, so-called 'surface darkening'. However, exploration into such decrease in albedo and its radiative and meteorological effects is still fairly limited. As one of the most high-yield agricultural areas, eastern China features straw burning every early summer, the harvest season for winter wheat, which was particularly strong in 2012. Satellite retrievals shows that surface albedo was significantly decreased (up to -0.16 decrease in the near-infrared broadband). Observational evidences of abnormal surface warming were found by comparing radiosonde and reanalysis data. Most sites around intensive burned scars, especially in the downwind direction shows a positive deviation. Comparisons between 'pre-fire' and 'post-fire' from 2007 to 2015 indicated a larger temperature bias of the forecast during 'post-fire' stage. The signal is more obvious in the later afternoon. WRF-Chem simulations suggest that including 'surface darkening' can decrease model bias and well captured temperature variation after burning at sites in fire areas and its adjacent area. This work highlights the importance of biomass burning induced albedo change in weather forecast and regional climate.

1 Introduction

Biomass burning (BB) refers to open or quasi-open combustion of plants or organic fuels, including prescribed burning, agricultural wastes burning and wildfires in forests and savannas and so on (Thompson, 1996;Andreae and Merlet, 2001;Andreae, 1991). BB can directly destruct vegetation covers and affect soil properties over fire prone areas (Certini, 2005), and is considered as one of the most important factors influencing the global terrestrial ecosystem (Fearnside, 2000). Large amount of particulate matter, trace gases, along with greenhouse gases released by BB can substantially modify the atmospheric chemical composition, degrade air quality, perturb radiation budget and then alter weather and climate significantly on local, regional and even global scale (Hobbs et al., 1997;Podgorny et al., 2003;Hansen, 2005;Haywood and Ramaswamy, 1998;Crutzen et al., 1979;Crutzen and Andreae, 1990;Langmann, 2009;Chan and Yao, 2008;Chen et al., 2017;Chang and Song, 2010). Intensive BB occurs across the world every year with significant seasonal and interannual

https://doi.org/10.5194/acp-2019-957
Preprint. Discussion started: 10 December 2019

Atmospheric Chemistry and Physics Discussions

variations and distinct regional characteristics (Duncan B. N.; Martin, 2003;Hao and Liu, 1994;Streets et al., 2003;Kaiser et al., 2012;Wiedinmyer et al., 2011;Uhl and Kauffman, 1990;Bowman and Panton, 1994), and bring about much human health loss, premature mortality and morbidity, especially in developing countries, which is an alarming situation (Pöschl, 2005;Qin et al., 2019;Wang et al., 2015;Wang et al., 2017). Though supervision has been strengthened, threats from global fire activities are still increasing dramatically with climatic and anthropogenic drivers (Marlon et al., 2009;Van Der Werf et al., 2006;Pechony and Shindell, 2010;Marshall et al., 1996;Penner et al., 1992).

Since open BB tends to occur directly on land surface, land cover and underlying surface properties would be affected straightway (Myhre et al., 2005;Certini, 2005). Surface albedo was revealed to be highly sensitive to BB, a sharp drop down to abnormally low values of which can be observed over fire prone areas due to the surface darkening caused by black charcoal produced in incomplete combustion, and will maintain for a period of time before char materials are removed by weathering and vegetation starts to regenerate (Jin and Roy, 2005;Govaerts et al., 2002;Myhre et al., 2005;Veraverbeke et al., 2012;Beringer et al., 2003;Bremer, 1999;Amiro et al., 2006;Govaerts et al., 2003;Tsuyuzaki et al., 2008;Lyons et al., 2008). The magnitude of such a decrease in surface albedo depends on fire intensity and can be up to half of pre-fire values (Veraverbeke et al., 2012). Reduction in surface albedo enhances the capacity of fire-affected surface to absorb solar radiation under clear sky condition, perturbing the surface energy budget and the process of land-atmosphere interaction, and then modifying local or even regional circulations (Govaerts et al., 2003;Gatebe et al., 2014). These changes in meteorological parameters will be important for weather and air quality forecast (Zhang et al., 2016;Ding et al., 2013a;Yang et al., 2019).

With the highest crop production in the world, about 122 Tg of crop residue are burned on spot annually in China in estimation (Streets et al., 2003). Eastern China, especially the middle and lower reaches of Yellow River and Yangtze River, features large plain area and dense population with high agricultural production. Owing to a distinctive rotation cycle of "winter wheat, summer maize", eastern China has been characterized by intensive straw burning every summer, especially June, the harvest season for winter wheat (Yin et al., 2019;Li et al., 2016;He et al., 2007;Huang et al., 2012a;Huang et al., 2018;Yang et al., 2013). After revolution in rural fuel structure, farmers who are eager to deal with tons of wheat straw and continue the cycle always resort to burning on spot rather than taking them as fuel. Hence, the wheat straw burning is exceedingly dense in both time and space, posing alarming threats to air quality and human health (Huang et al., 2012b;Nie et al., 2015;Ding et al., 2016a;Ding et al., 2016b;Ding et al., 2013a). The combination of BB emissions and fossil fuel emissions in eastern China also brings great challenges to weather and climate forecast (Xu et al., 2018;Zhou et al., 2018;Ding et al., 2013b;Wang et al., 2018).

An extremely typical pollution episode was triggered in eastern China in June 2012, when the most severe straw burning happened based on statistics (Huang et al., 2012b). A yellow haze blanketed the Yellow River Delta (YRD), resulting from intensive BB emissions from northern agricultural area mixed with local fossil fuel emissions (Xie et al., 2015;Ding et al., 2013a). During the episode, a series of meteorological anomalies were observed, such as air temperature changes and precipitation redistribution, which have been attributed to aerosols, particularly absorption aerosols like black carbon (BC)

https://doi.org/10.5194/acp-2019-957
Preprint. Discussion started: 10 December 2019

Atmospheric Chemistry and Physics Discussions

(Huang et al., 2016;Ding et al., 2013a;Gao et al., 2018). However, the impact of local and region energy budget, like surface darkening (Jin and Roy, 2005;Myhre et al., 2005) have not been depicted yet. The striking spectral contrast between dark charcoal deposit over burned surface and bright day ripening wheat could arouse distinct physical signals (Govaerts et al., 2003;Pereira et al., 1999). What's more, the effect of fire on albedo is complex and depends on the pre-fire structure, underlying soil reflectance, combustion completeness of fire and vegetation recovery after fire (Roy and Landmann, 2005). It also announces the urgent need of investigation in radiative and meteorological effects of fire-induced albedo change in eastern China combined with the high intensity of BB, especially in summer when solar radiation is extremely strong.

In this study, magnitude and distribution of surface albedo decrease induced by crop residue burning in eastern China, so called 'surface darkening' was investigated combining fire detections by MODIS based on straw burning in June 2012. Temperature anomalies after BB in eastern China were also explored using long-term site observations from 2007 to 2015, and comparisons were made between the two status, 'pre-fire' and 'post-fire'. Moreover, with the aid of the Weather Research and Forecasting model coupled with Chemistry (WRF-Chem model), decrease in surface albedo over fire prone areas were taken into consideration in the simulation targeting at temperature anomalies in June 2012. The further impact of 'surface darkening' in radiation budget, energy reallocation in Earth-atmosphere system and meteorology were discussed on a local and regional scale, which is of assignable climatological significance and should not be neglected.

2 Data and Method

2.1 Fire counts and surface albedo

The intensity of fire counts and magnitude of surface albedo decrease induced by crop residue burning were analyzed based on standard Moderate Resolution Imaging Spectroradiometer (MODIS) data products provided by NASA (Vermote, 2015;Giglio and Justice, 2015a, 2017, 2015b).

Surface Reflectance product MOD09A1 provides an estimate of the surface spectral reflectance of MODIS Band 1 through 7 at a horizontal resolution of 500 m and use Bidirectional Reflectance Distribution Function (BRDF) database to better constrain the different threshold used (Schaaf et al., 2002). The seven-narrowband albedo can be converted to broadband like shortwave and near-infrared through valid algorithms (Liang, 2001;Liang et al., 2003). It has been corrected for atmospheric conditions such as gases, aerosols and Rayleigh scattering. The dataset is updated every 8 d, for selecting one value from all acquisitions in an 8-day composite period for each pixel unit. The criteria for grid cell value selection includes cloud conditions and solar zenith angle.

Thermal Anomalies/Fire Daily L3 Global product (MOD/MYD14A1) combined with burned area product (MCD64A1) were adopted to determine the locations and time of burning and mark the burned scar. MOD14A1 and MYD141 are daily surface thermal anomaly data obtained by Terra and Aqua satellites with spatial resolution of 1000m, and fire counts with low confidence were counted out for quality control (Hawbaker et al., 2008). MCD64A1 Burned Area data product is monthly upgraded and contains burned date and quality information for each pixel, using burn sensitive vegetation index (VI) derived

https://doi.org/10.5194/acp-2019-957
Preprint. Discussion started: 10 December 2019


Atmospheric Chemistry and Physics Discussions

from atmospherically corrected surface albedo information of MODIS short-wave infrared band to create dynamic thresholds for composite data (Giglio et al., 2016;Giglio et al., 2009). The “fire count" described in the following part indicates the central location of MODIS pixels with surface thermal anomalies. The actual geographic size of the pixel varies depending on the angle at which satellite scans. When counting the number of pixels in target region, the pixels are abstracted into points on a two-dimensional plane.

2.2 Temperature observation and forecast

Meteorological sites observations from National Centers for Environmental Information (NCEI) offer the hourly air temperature at 2 m height, while atmospheric sounding observation at Xuzhou station is provided by University of Wyoming (http://weather.uwyo.edu/upperair/sounding.html).The temperature observations were used to compare with National Centers for Environmental Prediction (NCEP) global final analysis data (FNL) with a $1° \times 1°$ spatial resolution which is updated every 6 h, and were also applied for verification and analysis of numerical simulations.

2.3 Experiment design and model configuration

WRF-Chem version 3.6.1, an online-coupled chemical transport model, was adopted in this study, in which multiple physical and chemical processes are depicted including emission, transport, mixing, and chemical transformation of trace gases and aerosols simultaneously with meteorology (Grell et al., 2005).

In order to take fire-induced albedo change into consideration and figure impact of ‘surface darkening’ in radiation budget and meteorology in eastern China, a pair of parallel experiments in WRF-Chem with surface albedo as variable was designed: In CTL run, default value of monthly surface albedo in model was adopted, while in ABD run, surface albedo was set by subtracting a certain value from the default model value over fire-prone areas. The fire-prone areas were extracted out based on density of fire counts in June 2012, and the certain value characterizing the magnitude of albedo decrease were defined based on satellite data analysis in Section 3.1.

The initial and lateral boundary conditions of meteorological variables are obtained from NCEP FNL that update every 6 h. MIX, a mosaic Asian anthropogenic emission inventory developed by Tsinghua University (Li et al., 2017)and the Fire Inventory from NCAR (FINN) providing high resolution global emission estimates from open burning (Wiedinmyer et al., 2011) were applied in WRF-Chem as anthropogenic and BB emissions, respectively. The simulations were conducted for the time period 2-18 June 2012, and was split into eight independent 72-h runs for the meteorological fields, while the chemical outputs from the preceding run were used as the initial conditions for the following run. Only the last 48 h results of each run were kept for analysis, and the first 7 d were regarded as the model spin-up period for atmospheric chemistry, so as to allow the model to reach a state of statistical equilibrium under the applied forcing (Lo et al., 2008;Berge et al., 2001).

Moreover, since the experiments were designed on the basis of MOIDS products simulation, the MODIS surface classification options of the International Geosphere-Biosphere Programme (IGBP) and the matched Noah land surface

https://doi.org/10.5194/acp-2019-957
Preprint. Discussion started: 10 December 2019


Atmospheric Chemistry and Physics Discussions

scheme was adopted in CTL and ABD to keep consistency. The specific settings of domain and parameterization schemes in both CTL and ABD are listed in Table 1.

3 Results and discussion

3.1 Fire-induced surface albedo change

In 2012, the total mass of crop residue burned was 160 Tg, and 38,053 fires were recorded on farmland accounting for 36% of the total and most occurred in June, the harvest season for wheat (Li et al., 2016). Yellow-Huai River areas (YHR), located in the vast flat plain in eastern China, is the major wheat producing area in China. Figure 1a shows the daily agricultural MODIS fire counts in YHR, where cropland especially wheat fields dominates vegetation cover (Gong et al., 2019;Van Der Werf et al., 2010;Li et al., 2016). The limited duration of agricultural fire combined with the low temporal resolution of MODIS may increase the difficulty of signal capture and lead to underestimation of fire counts (Randerson et al., 2012;Li et al., 2016;Giglio et al., 2009;Chang and Song, 2010, 2009). As illustrated in Fig. 1a, severe and intensive BB events happened in mid-early June, especially 7-13 June, a tense and busy period in the crop cycle for harvest of wheat and sowing of maize. Among them, burning on 13 June is the most serious. Black charcoal deposit produced in high-intensive open straw burning would adhere to exposed soil and bound surface albedo over a period of time before removal of char by natural process or regeneration of vegetation (Veraverbeke et al., 2012). The strong spectral contrast between dark burned surface and original bright dry ripening wheat cover can arouse distinct physical signals (Govaerts et al., 2003;Pereira et al., 1999).

Understanding the saliency and persistence of signals is important for estimation of albedo change amplitude and further analysis of its radiative and meteorological effects. The signals of ‘surface darkening’ was a relatively short duration for about one week and much more sensitive in shortwave near-infrared bands (Trigg and Flasse, 2000). Considering higher resolution and better depiction of narrow-band satellite observations, and the outstanding capacity of near-infrared to separate the signals between vegetation and charcoal (Jin and Roy, 2005;Trigg and Flasse, 2000), MODIS Narrow-band2 (shortwave near-infrared, from 0.841 μm to 0.876 μm) was chosen. Figure 1b and 1c show the surface albedo distribution before and after the severe burning season separately, based on MOD09A1 dataset which updates every 8 d and has ruled out the interference of clouds. Distribution on 1 June has not been adopted for high missing data rate. For MODIS narrow band2, decrease induced by fire is about 0.30 to 0.14 in zone YHR, almost half of original values. The immediate surface albedo decrease after fire can be attributed to the large-scale replacement of ripening wheat with black charcoal over fire prone areas, so-called ‘burned scar’. Char materials strongly absorb the incoming sunlight and as such and cause a significant reduction of the reflection-to-incoming sunlight ratio (Veraverbeke et al., 2012), so burning like this could disturb surface radiation balance at a level that cannot be ignored, which needs further exploration.

The distribution accumulated high-confidence fire counts during the highly intensive straw-burning in June 2012 is shown in Fig. 2a, with an exactly same time window as Fig. 1b and 1c, from 24 May to 17 June. Combined, surface albedo changes

https://doi.org/10.5194/acp-2019-957
Preprint. Discussion started: 10 December 2019


Atmospheric Chemistry and Physics Discussions

during the same period over fire prone areas obtained by MODIS in shortwave near-infrared broadband are shown in Fig. 2b, in accordance with the location of fire counts. As illustrated, fire counts are fairly concentrated in zone YHR, the major wheat-producing area on the eastern China plain. Correspondingly, extensive negative values in Fig. 2b demonstrate substantial reduction of surface albedo over fire prone area in zone YHR, especially where fire counts are the densest. For near-infrared broadband, decrease ranges in -0.02 ~ -0.16. Though the MODIS surface albedo dataset applied here has ruled out cloud interference, partial inevitable noises like cloud shadow still exist, reflecting on the scattering positive values in the north-western region in Fig. 2b.

To further explore the radiative and meteorological effects of 'surface darkening' and provide a basis for the following numerical experiments, frequency distributions of surface albedo decrease in near-infrared and short-wave are shown in Fig. 3, to clarify the magnitude of surface albedo decrease. The sample size of fire counts is 9,477 pixels, consistent with those marked in Fig. 2a. Surface albedo change in most fire-affected pixels changes distribute in negative region, while the noises in positive area correspond to those larger positive values in the north-western region in Fig. 2b owing to cloud shadows. The peaks are relatively flat for both near-infrared and shortwave, and peak values for shortwave distribute between -0.02 and -0.06, for near-infrared distribute between -0.06 and -0.10. Since nearly half of the solar energy that reaches the surface is at wavelengths longer than 0.7 μm, albedo change in near-infrared is rather significant for the energy budget of the surface (Hartmann, 1994). According to the above analysis, in Section 3.3, the certain value of surface albedo decrease adopted in ABD run was -0.1 to examine the disturbance on surface energy budget and its potential regional meteorology impacts.

3.2 Observational evidences on surface warming in 'post-fire' period

Surface albedo is defined as the fraction of the downward solar flux density that is reflected by the surface, directly determining the absorptivity of the surface (Hartmann, 1994). Under the condition with same downward solar flux at the surface, decrease in albedo more solar radiation will be absorbed. Without any plants doing photosynthesis over fire prone areas, the immediate fire-induced increase in absorption of radiative energy are used to heat the ground mostly and then warm the near surface atmosphere (Andrews, 2010;Wallace and Hobbs, 2006), which could lead to a phenomenon of surface warming. What's more, solar radiation is the strongest in summer when straw burning bursts in YHR, and the response of surface albedo can be the fiercest. Hence, the air temperature observations over fire prone areas after BB were investigated.

Near-surface air temperature observations at meteorological sites were compared with FNL data in 2012. Refer to Fig. 1a, burning in zone YHR is the most severe on 13 June, while 18 June is the end date of the wheat straw burning 'season' in 2012. Temperature bias at 2 m height in observational network at 20:00 LT on 13 and 18 June was shown in Fig. 4, filled according to the value of observation minus FNL. In addition, fire counts on the day and accumulated during past five days, so called 'burned scar', were marked. The scattered positive values of temperature bias in Fig. 4 represent that observational temperature at those sites are higher than predictions from forecast model with only a small fraction of assimilated observations. Most sites around intensive burned scars, especially in the downwind direction shows a positive deviation, which is an abnormal signal of surface warming.

https://doi.org/10.5194/acp-2019-957
Preprint. Discussion started: 10 December 2019


Atmospheric Chemistry and Physics Discussions

In fact, intensive straw burning occurred in the zone YHR every June during the harvest of wheat over the past twenty years before strict regulation launched in recent years (Yin et al., 2019;Li et al., 2016), which could announce significance in climatology to understand the signals of surface warming after BB.

Xuzhou station (marked in Fig. 4), the only sounding site located in the most intensive fire prone area in zone YHR. Sounding observations at Xuzhou from 2007 to 2015 was compared with FNL data in the planet boundary layer. Sample of days was selected out according to burning condition in each year, and has been classified into specific status, 'pre-fire' and 'post-fire'. 'Post-fire' days must be in 5 days after a severe burning, while 'pre-fire' must be among the 5 days before fire but not in 5 days after previous fire. Only days under clear sky condition were selected. The statistical distribution of temperature bias on different isobaric levels at 20:00 LT in the two status was shown in Fig. 5a and 5b. Temperature bias was defined as the value of sounding observation minus FNL data. As illustrated, temperature biases are mostly positive on the lower levels in both two status, and absolute values of 'post-fire' are larger than 'pre-fire'. Combined with Fig. 5c, it means observations at 'post-fire' have bigger positive deviation from forecast results, a signal of abnormal warming at 'post-fire'. In addition, with regards to the vertical profile of bias at 'post-fire' (Fig. 5b), deviations on lower levels tend to be bigger and more positive than those on higher levels. Sounding data updates 2 times a day, 08:00 LT and 20:00 LT, and only patterns at 20:00 LT was shown here since no significance difference exists between the two status at 08:00 LT. Under clear sky condition, the thermal states near the ground level have passed through radiation absorption and accumulation during daytime by 20:00 LT. The abnormal warming signal that tends to be more obvious near the surface, can be explained as the enhancement of surface heat absorptivity by decrease in surface albedo.

For the same sample of days in 2007-2015, the diurnal variation of 2-m temperature bias between site observations and FNL, in the two status was shown in Fig. 6 by box plot. Negative values of deviation at 08:00 LT and 14:00 LT show that FNL tends to overestimate temperature during daytime and underestimate at night. It is noteworthy that the absolute deviation of 'post-fire' is always larger than 'pre-fire' no matter during the day or night, which means decrease in predictability of temperature at 'post-fire'. With regard to the median values, bias goes through the process of a gradually surpass over 'pre-fire', consistent with the warming signal revealed by sounding analysis at Xuzhou at 20:00 LT. The continuous rising tendency during the daytime demonstrates a needed response time of heat accumulation, which may be attributed to the radiative effect of 'surface darkening' (Myhre et al., 2005;Andrews, 2010). So, the signal of abnormal warming is more obvious in the later afternoon and early evening.

3.3 Improved temperature simulation by considering surface albedo change

As aforementioned, fire-induced surface albedo change and observational evidences of abnormal surface warming were substantial in eastern China. However, the possible radiative effects on local or regional meteorology and the behind physical images has not been figured out yet, which should resort to model simulation. Moreover, YHR is just adjacent to the Yangtze River Delta, an economic and cultural centre in Asia with worldwide concern, which emphasizing the knowledge of the regional impacts of albedo change. In existing studies, radiative effects of albedo changes over burned

https://doi.org/10.5194/acp-2019-957
Preprint. Discussion started: 10 December 2019


Atmospheric Chemistry and Physics Discussions

scars were investigated on different land covers, like boreal forest (Lyons et al., 2008) and savanna (Myhre et al., 2005;Jin and Roy, 2005), but few of them was conducted on agricultural fire in production areas.

Hence, WRF-Chem experiments targeting at surface albedo change induced by agricultural BB in eastern China were conducted. The most severe episode happened in June 2012 was selected as the case. Distributions of the two parallel experiments, CTL and ABD, were shown in Fig. 7a and 7b. The surface albedo decrease over fire prone areas was set to 0.1. Model results were compared with site observational air temperature, respectively in concentrated fire prone areas (Fig. 8a) and its southern adjacent area, YRD (Fig. 8b). In Fig. 8, results of ABD show temperature increase and enjoy a better fit with observations at both sites in afternoon and early evening compared to CTL. Temperature anomalies can be simulated to some extent, after considering the decrease in surface albedo caused by BB.

The local surface energy budget at Bengbu was shown in Fig. 9. Bengbu locates in fire affected area where adopted the decreased albedo. As shown in Fig. 9a, upward shortwave radiation at the surface reduces a lot, while only a little change exists in downward shortwave radiation reaching surface. The smaller ratio of solar radiation reflected to the atmosphere by surface can be attributed surface albedo decrease. Accordingly, with more solar radiation absorbed by surface, the ground will be heated and the surface temperature will be higher in ABD (Fig. 9b). Higher surface temperature would give rise to larger upward heat flux, thereby heating the atmosphere near the surface (Stull, 1988). So, local radiation budget change induced by surface albedo change would directly influence the near-surface air temperature and arouse an abnormal warming signal over fire prone areas in the afternoon and early evening with a certain lag.

Meanwhile, the warming effect of fire-induced albedo change is also obvious in adjacent areas like Lukou (Fig. 8b), located in south of Nanjing. Some other stations like Wuhu and Liyang in YRD also show similar patterns. Considering that local temperature change is affected by various factors such as local radiation budget change and advection transport caused by thermal disturbance. As illustrated in Fig. 10a, surface warming shows in the upwind area of Lukou station, which means influence of warm advection. According to Fig. 10b and 10c, sharp decrease in low cloud water contents was found in the upwind area. Low clouds are very effective reflectors of solar radiation (Hartmann, 1994), giving rise to large perturbations to surface radiation budget. In Fig. 10d, downward shortwave reaching the surface in ABD reduces quit a lot due to reflection and occlusion of low clouds. Since surface over fire prone areas are additionally heated, surface temperature increases, and both sensible heat flux and latent heat flux will be changed which could arouse variation in boundary layer like vertical velocity and disturb the cloud formation (Stull, 1988). Decrease in surface albedo over fire prone area can also has great impact on adjacent areas where surface albedo was barely changed by disturbance to cloud formation and advection transmission.

'Burned scar' can remain over the surface for about one week under rainy condition or even longer if dryer and calmer (Trigg and Flasse, 2000). The length of period allows the process of local radiative accumulation and disturbance in regional circulation, and influence on temperature in both fire prone area and adjacent areas.

https://doi.org/10.5194/acp-2019-957
Preprint. Discussion started: 10 December 2019

Atmospheric Chemistry and Physics Discussions

4 Conclusions

To figure out the change in surface albedo induced by biomass burning and its impact on regional meteorology in eastern China, an investigation into the relationship between surface albedo change and temperature anomalies was conducted based on meteorological observations and satellite retrievals, combining with WRF-Chem simulations. This study focuses on the intensive wheat straw burning occurred in the YHR area, the major wheat producing area of eastern China, in early summer. The most severe and classic burning episode in 2012 was chosen to be the case.

Fire-induced surface albedo change was verified in YHR area based on satellite retrievals. Large area of "surface darkening" shows over fire prone area. In the near-infrared broadband, the absolute albedo decreased ranges in -0.16 ~ -0.02, which can be an obvious signal in the regional scale and arouse large radiative disturbance. Peak values of reduction for shortwave distributed between -0.06 and -0.02, for near-infrared distribute between -0.10 and -0.06.

Evidences of abnormal surface warming were found in eastern China. Most sites around intensive burned scars, especially in the downwind direction shows a positive deviation in June 2012, which is an abnormal signal of surface warming. Comparisons were made between status of 'pre-fire' and 'post-fire' under clear sky condition, based on multi-years temperature observations from 2007 to 2015. Observations at 'post-fire' have bigger positive deviation from forecast results, especially on lower levels, which is a signal of abnormal surface warming at 'post-fire' and decrease in predictability. The signal is more obvious in the later afternoon and early evening.

To examine the direct radiative effects and its potential regional meteorological impacts of surface albedo change, WRF-Chem experiments targeting at the surface albedo change induced by agricultural BB in eastern China were carried out. Results of experiment ABD show temperature increase and enjoy a better fit with observations at both sites in concentrated fire prone areas and its southern adjacent area compared to CTL, especially in afternoon and early evening. Surface albedo change over fire prone areas influence the surface temperature through direct local radiation budget change and indirect disturbance in cloud formation and advection transmission.

This study shows that either human or natural induced biomass burning will not only influence the weather and regional climate by emission of aerosols and trace gases. The change in surface albedo could also cause significant impacts at regional scale during the post-fire periods, particular in regions with strong solar radiation. Such kind of short-term disturbance should be considered in future weather, climate and air quality forecast models.

Data availability. Meteorological datasets used in this work can be acquired from https://rda.ucar.edu/datasets/ds083.2/, http://weather.uwyo.edu/upperair/sounding.html, and https://www7.ncdc.noaa.gov/CDO/cdoselect.cmd. MODIS dataset can be obtained from the Level-1 and Atmosphere Archive & Distribution System (LAADS) Distributed Active Archive Center (DAAC), located in the Goddard Space Flight Center in Greenbelt, Maryland (https://ladsweb.nascom.nasa.gov).

https://doi.org/10.5194/acp-2019-957
Preprint. Discussion started: 10 December 2019

Atmospheric Chemistry and Physics Discussions

Author contributions. RT and XH led the manuscript writing. RT and DZ conducted the data analysis and model simulations. AD contributed to the research design.

Competing interests. The authors declare that they have no conflict of interest.

Acknowledgements. This work was supported by the National Natural Science Foundation of China (91544231, 41725020, 91744311, and 41422504). The numerical modeling was conducted on computing facilities at the High Performance Computing Centering (HPCC) at Nanjing University.

References

Amiro, B. D., Orchansky, A. L., Barr, A. G., Black, T. A., Chambers, S. D., Chapin Iii, F. S., Goulden, M. L., Litvak, M., Liu, H. P., McCaughey, J. H., McMillan, A., and Randerson, J. T.: The effect of post-fire stand age on the boreal forest energy balance, AGR FOREST METEOROL, 140, 41-50, 10.1016/j.agrformet.2006.02.014, 2006.

Andreae, M. O.: Biomass burning - its history, use, and distribution and its impact on environmental-quality and global climate, Global Biomass Burning: Atmospheric, Climatic, and Biospheric Implications, edited by: Levine, J. S., M I T Press, Cambridge, 3-21 pp., 1991.

Andreae, M. O., and Merlet, P.: Emission of trace gases and aerosols from biomass burning, GLOBAL BIOGEOCHEM CY, 15, 955-966, 10.1029/2000gb001382, 2001.

Andrews, D. G.: An Introduction to Atmospheric Physics, Cambridge University Press, 2010.

Berge, E., Huang, H. C., Chang, J., and Liu, T. H.: A study of the importance of initial conditions for photochemical oxidant modeling, J GEOPHYS RES-ATMOS, 106, 1347-1363, 10.1029/2000jd900227, 2001.

Beringer, J., Hutley, L. B., Tapper, N. J., Coutts, A., Kerley, A., and O'Grady, A. P.: Fire impacts on surface heat, moisture and carbon fluxes from a tropical savanna in northern Australia, INT J WILDLAND FIRE, 12, 333-340, 10.1071/wf03023, 2003.

Bowman, D., and Panton, W. J.: Fire and cyclone damage to woody vegetation on the north coast of the northern-territory, australia, AUST. GEOGR., 25, 32-35, 10.1080/00049189408703096, 1994.

Bremer, D. J. H., J. M.: Effect of spring burning on the surface energy balance in a tallgrass prairie, AGR FOREST METEOROL, 97, 43-54, 10.1016/s0168-1923(99)00034-9, 1999.

Certini, G.: Effects of fire on properties of forest soils: a review, OECOLOGIA, 143, 1-10, 10.1007/s00442-004-1788-8, 2005.

Chan, C. K., and Yao, X.: Air pollution in mega cities in China, ATMOS ENVIRON, 42, 1-42, 10.1016/j.atmosenv.2007.09.003, 2008.

Chang, D., and Song, Y.: Comparison of L3JRC and MODIS global burned area products from 2000 to 2007, 114, 10.1029/2008jd011361, 2009.

Chang, D., and Song, Y.: Estimates of biomass burning emissions in tropical Asia based on satellite-derived data, 10, 2335-2351, 10.5194/acp-10-2335-2010, 2010.

Chen, J. M., Li, C. L., Ristovski, Z., Milic, A., Gu, Y. T., Islam, M. S., Wang, S. X., Hao, J. M., Zhang, H. F., He, C. R., Guo, H., Fu, H. B., Miljevic, B., Morawska, L., Thai, P., Fat, L., Pereira, G., Ding, A. J., Huang, X., and Dumka, U. C.: A review of biomass burning:

https://doi.org/10.5194/acp-2019-957
Preprint. Discussion started: 10 December 2019

Emissions and impacts on air quality, health and climate in China, SCI TOTAL ENVIRON, 579, 1000-1034, 10.1016/j.scitotenv.2016.11.025, 2017.

Crutzen, P. J., Heidt, L. E., Krasnec, J. P., Pollock, W. H., and Seiler, W.: Biomass burning as a source of atmospheric gases CO, H2, N2O, NO, CH3Cl and COS, Nature, 282, 253-256, 10.1038/282253a0, 1979.

Crutzen, P. J., and Andreae, M. O.: Biomass burning in the tropics - impact on atmospheric chemistry and biogeochemical cycles, Science, 250, 1669-1678, 10.1126/science.250.4988.1669, 1990.

Ding, A. J., Fu, C. B., Yang, X. Q., Sun, J. N., Petäjä, T., Kerminen, V. M., Wang, T., Xie, Y., Herrmann, E., Zheng, L. F., Nie, W., Liu, Q., Wei, X. L., and Kulmala, M.: Intense atmospheric pollution modifies weather: a case of mixed biomass burning with fossil fuel combustion pollution in eastern China, 13, 10545-10554, 10.5194/acp-13-10545-2013, 2013a.

Ding, A. J., Fu, C. B., Yang, X. Q., Sun, J. N., Zheng, L. F., Xie, Y. N., Herrmann, E., Nie, W., Petäjä, T., Kerminen, V. M., and Kulmala, M.: Ozone and fine particle in the western Yangtze River Delta: an overview of 1 yr data at the SORPES station, ATMOS CHEM PHYS, 13, 5813-5830, 10.5194/acp-13-5813-2013, 2013b.

Ding, A. J., Huang, X., Nie, W., Sun, J. N., Kerminen, V. M., Petäjä, T., Su, H., Cheng, Y. F., Yang, X. Q., Wang, M. H., Chi, X. G., Wang, J. P., Virkkula, A., Guo, W. D., Yuan, J., Wang, S. Y., Zhang, R. J., Wu, Y. F., Song, Y., Zhu, T., Zilitinkevich, S., Kulmala, M., and Fu, C. B.: Enhanced haze pollution by black carbon in megacities in China, GEOPHYS RES LETT, 43, 2873-2879, 10.1002/2016gl067745, 2016a.

Ding, A. J., Nie, W., Huang, X., Chi, X., Sun, J., Kerminen, V.-M., Xu, Z., Guo, W., Petäjä, T., Yang, X., Kulmala, M., and Fu, C.: Long-term observation of air pollution-weather/climate interactions at the SORPES station: a review and outlook, Frontiers of Environmental Science & Engineering, 10, 10.1007/s11783-016-0877-3, 2016b.

Duncan B. N.; Martin, R. V. S. A. C. Y. R. L. J. A.: Interannual and seasonal variability of biomass burning emissions constrained by satellite observations, J GEOPHYS RES, 108, 10.1029/2002jd002378, 2003.

Fearnside, P. M.: Greenhouse gas emissions from land-use change in Brazil's Amazon region, Global Climate Change and Tropical Ecosystems, edited by: Lal, R., Kimble, J. M., and Stewart, B. A., Crc Press-Taylor & Francis Group, Boca Raton, 231-249 pp., 2000.

Gao, M., Ji, D. S., Liang, F. C., and Liu, Y.: Attribution of aerosol direct radiative forcing in China and India to emitting sectors, ATMOS ENVIRON, 190, 35-42, 10.1016/j.atmosenv.2018.07.011, 2018.

Gatebe, C. K., Ichoku, C. M., Poudyal, R., Román, M. O., and Wilcox, E.: Surface albedo darkening from wildfires in northern sub-Saharan Africa, ENVIRON RES LETT, 9, 065003, 10.1088/1748-9326/9/6/065003, 2014.

Giglio, L., Loboda, T., Roy, D. P., Quayle, B., and Justice, C. O.: An active-fire based burned area mapping algorithm for the MODIS sensor, 113, 408-420, 10.1016/j.rse.2008.10.006, 2009.

Giglio, L., Schroeder, W., and Justice, C. O.: The collection 6 MODIS active fire detection algorithm and fire products, REMOTE SENS ENVIRON, 178, 31-41, 10.1016/j.rse.2016.02.054, 2016.

Gong, P. L., H.; Zhang, M. N.; Li, C. C.; Wang, J.; Huang, H. B.; Clinton, Nicholas; Ji, L.Y.; Li, W.Y.; , Bai, Y., Chen, B., Xu, B., Zhu, Z., Yuan, C., Ping Suen, H., Guo, J., Xu, N., Li, W., Zhao, Y., Yang, J., Yu, C., Wang, X., Fu, H., Yu, L., Dronova, I., Hui, F., Cheng, X., Shi, X., Xiao, F., Liu, Q., and Song, L.: Stable classification with limited sample: transferring a 30-m resolution sample set collected in 2015 to mapping 10-m resolution global land cover in 2017, SCI BULL, 64, 370-373, 10.1016/j.scib.2019.03.002, 2019.

Govaerts, Y. M., M., P. J., B., P., and B., M.: Impact of fires on surface albedo dynamics over the African continent, J GEOPHYS RES, 107, 10.1029/2002jd002388, 2002.

https://doi.org/10.5194/acp-2019-957
Preprint. Discussion started: 10 December 2019

Govaerts, Y. M., Pinty, B., and Lattanzio, A.: Impact of vegetation fires on surface albedo dynamics and absorbed solar radiation over the African Continent, 3, 1576-1578, 10.1109/igarss.2003.1294180, 2003.

Grell, G. A., Peckham, S. E., Schmitz, R., McKeen, S. A., Frost, G., Skamarock, W. C., and Eder, B.: Fully coupled "online" chemistry within the WRF model, ATMOS ENVIRON, 39, 6957-6975, 10.1016/j.atmosenv.2005.04.027, 2005.

Hansen, J.: Efficacy of climate forcings, 110, 10.1029/2005jd005776, 2005.

Hao, W. M., and Liu, M.-H.: Spatial and temporal distribution of tropical biomass burning, GLOBAL BIOGEOCHEM CY, 8, 495-503, 10.1029/94gb02086, 1994.

Hartmann, D. L.: Global Physical Climatology, Academic Press, 1994.

Hawbaker, T. J., Radeloff, V. C., Syphard, A. D., Zhu, Z. L., and Stewart, S. I.: Detection rates of the MODIS active fire product in the United States, REMOTE SENS ENVIRON, 112, 2656-2664, 10.1016/j.rse.2007.12.008, 2008.

Haywood, J. M., and Ramaswamy, V.: Global sensitivity studies of the direct radiative forcing due to anthropogenic sulfate and black carbon aerosols, J GEOPHYS RES-ATMOS, 103, 6043-6058, 10.1029/97jd03426, 1998.

He, L. M., Wang, W. J., Q., W., B., W., Q., L., Z., W. C., and M., L. X.: Evaluation of the Agricultural Residues Burning Reduction in China Using MODIS Fire Product, Environmental Monitoring in China, 23, 42-50, 2007.

Hobbs, P. V., Reid, J. S., Kotchenruther, R. A., Ferek, R. J., and Weiss, R.: Direct radiative forcing by smoke from biomass burning, Science, 275, 1776-1778, 1997.

Huang, X., Li, M. M., Li, J. F., and Song, Y.: A high-resolution emission inventory of crop burning in fields in China based on MODIS Thermal Anomalies/Fire products, ATMOS ENVIRON, 50, 9-15, 10.1016/j.atmosenv.2012.01.017, 2012a.

Huang, X., Song, Y., Li, M. M., Li, J. F., and Zhu, T.: Harvest season, high polluted season in East China, ENVIRON RES LETT, 7, 044033, 10.1088/1748-9326/7/4/044033, 2012b.

Huang, X., Ding, A. J., Liu, L. X., Liu, Q., Ding, K., Niu, X. R., Nie, W., Xu, Z., Chi, X. G., Wang, M. H., Sun, J. N., Guo, W. D., and Fu, C. B.: Effects of aerosol–radiation interaction on precipitation during biomass-burning season in East China, ATMOS CHEM PHYS, 16, 10063-10082, 10.5194/acp-16-10063-2016, 2016.

Huang, X., Wang, Z. L., and Ding, A. J.: Impact of Aerosol-PBL Interaction on Haze Pollution: Multiyear Observational Evidences in North China, GEOPHYS RES LETT, 45, 8596-8603, 10.1029/2018gl079239, 2018.

Jin, Y., and Roy, D. P.: Fire-induced albedo change and its radiative forcing at the surface in northern Australia, GEOPHYS RES LETT, 32, 10.1029/2005gl022822, 2005.

Kaiser, J. W., Heil, A., Andreae, M. O., Benedetti, A., Chubarova, N., Jones, L., Morcrette, J. J., Razinger, M., Schultz, M. G., Suttie, M., and Van Der Werf, G. R.: Biomass burning emissions estimated with a global fire assimilation system based on observed fire radiative power, BIOGEOSCIENCES, 9, 527-554, 10.5194/bg-9-527-2012, 2012.

Langmann, B. D., B. ; Textor, C.; Trentmann, J.; Van Der Werf, G. R.: Vegetation fire emissions and their impact on air pollution and climate, ATMOS ENVIRON, 43, 107-116, 10.1016/j.atmosenv.2008.09.047, 2009.

Li, J., Bo, Y., and Xie, S. D.: Estimating emissions from crop residue open burning in China based on statistics and MODIS fire products, J ENVIRON SCI, 44, 158-170, 10.1016/j.jes.2015.08.024, 2016.

Li, M., Zhang, Q., Kurokawa, J., Woo, J. H., He, K. B., Lu, Z. F., Ohara, T., Song, Y., Streets, D. G., Carmichael, G. R., Cheng, Y. F., Hong, C. P., Huo, H., Jiang, X. J., Kang, S. C., Liu, F., Su, H., and Zheng, B.: MIX: a mosaic Asian anthropogenic emission inventory under the international collaboration framework of the MICS-Asia and HTAP, ATMOS CHEM PHYS, 17, 935-963, 10.5194/acp-17-935-2017, 2017.

https://doi.org/10.5194/acp-2019-957
Preprint. Discussion started: 10 December 2019

Liang, S. L.: Narrowband to broadband conversions of land surface albedo I, REMOTE SENS ENVIRON, 76, 213-238, 10.1016/s0034-4257(00)00205-4, 2001.

Liang, S. L., Shuey, C. J., Russ, A. L., Fang, H. L., Chen, M. Z., Walthall, C. L., Daughtry, C. S. T., and Hunt, R.: Narrowband to broadband conversions of land surface albedo: II. Validation, 84, 25-41, 10.1016/s0034-4257(02)00068-8, 2003.

Lo, J. C. F., Yang, Z. L., and Pielke, R. A.: Assessment of three dynamical climate downscaling methods using the Weather Research and Forecasting (WRF) model, J GEOPHYS RES-ATMOS, 113, 16, 10.1029/2007jd009216, 2008.

Lyons, E. A., Jin, Y. F., and Randerson, J. T.: Changes in surface albedo after fire in boreal forest ecosystems of interior Alaska assessed using MODIS satellite observations, J GEOPHYS RES-BIOGEO, 113, n/a-n/a, 10.1029/2007jg000606, 2008.

Marlon, J. R., Bartlein, P. J., Carcaillet, C., Gavin, D. G., Harrison, S. P., Higuera, P. E., Joos, F., Power, M. J., and Prentice, I. C.: Erratum: Climate and human influences on global biomass burning over the past two millennia, NAT GEOSCI, 2, 307-307, 10.1038/ngeo468, 2009.

Marshall, S., Taylor, J. A., Oglesby, R. J., Larson, J. W., and Erickson, D. J.: Climatic effects of biomass burning, ENVIRON SOFTW, 11, 53-58, 10.1016/s0266-9838(96)00039-1, 1996.

Myhre, G., Govaerts, Y., Haywood, J. M., and K., B. T.: Radiative effect of surface albedo change from biomass burning, GEOPHYS RES LETT, 32, 10.1029/2005gl022897, 2005.

Nie, W., Ding, A. J., Xie, Y. N., Xu, Z., Mao, H., Kerminen, V. M., Zheng, L. F., Qi, X. M., Huang, X., Yang, X. Q., Sun, J. N., Herrmann, E., Petäjä, T., Kulmala, M., and Fu, C. B.: Influence of biomass burning plumes on HONO chemistry in eastern China, ATMOS CHEM PHYS, 15, 1147-1159, 10.5194/acp-15-1147-2015, 2015.

Pechony, O., and Shindell, D. T.: Driving forces of global wildfires over the past millennium and the forthcoming century, PNAS, 107, 19167-19170, 10.1073/pnas.1003669107, 2010.

Penner, J. E., Dickinson, R. E., and Neill, C. A.: Effects of aerosol from biomass burning on the global radiation budget, Science (New York, N.Y.), 5062, 1992.

Pereira, J. M. C., Sá, A. C. L., Sousa, A. M. O., Silva, J. M. N., Santos, T. N., and Carreiras, J. M. B.: Spectral characterisation and discrimination of burnt areas, 1999.

Podgorny, I. A., Li, F., and Ramanathan, V.: Large Aerosol Radiative Forcing due to the 1997 Indonesian Forest Fire, 30, 10.1029/2002gl015979, 2003.

Pöschl, U.: Atmospheric Aerosols: Composition, Transformation, Climate and Health Effects, ANGEW CHEM INT EDIT, 44, 7520-7540, 10.1002/anie.200501122, 2005.

Qin, Y., Fang, Y. Y., Li, X. Y., Naik, V., Horowitz, L. W., Liu, J. F., Scovronick, N., and Mauzerall, D. L.: Source Attribution of Black Carbon Affecting Regional Air Quality, Premature Mortality and Glacial Deposition in 2000, ATMOS ENVIRON, 2019.

Randerson, J. T., Chen, Y., van der Werf, G. R., Rogers, B. M., and Morton, D. C.: Global burned area and biomass burning emissions from small fires, J GEOPHYS RES-BIOGEO, 117, n/a-n/a, 10.1029/2012jg002128, 2012.

Roy, D. P., and Landmann, T.: Characterizing the surface heterogeneity of fire effects using multi-temporal reflective wavelength data, INT J REMOTE SENS, 26, 4197-4218, 10.1080/01431160500112783, 2005.

Schaaf, C. B., Gao, F., Strahler, A. H., Lucht, W., Li, X. W., Tsang, T., Strugnell, N. C., Zhang, X. Y., Jin, Y. F., Muller, J., Lewis, P., Barnsley, M., Hobson, P., Disney, M., Roberts, G., Dunderdale, M., Doll, C., D'Entremont, R. P., Hu, B., Liang, S., Privette, J. L., and Roy, D.: First operational BRDF, albedo nadir reflectance products from MODIS, REMOTE SENS ENVIRON, 83, 135-148, 10.1016/s0034-4257(02)00091-3, 2002.

https://doi.org/10.5194/acp-2019-957
Preprint. Discussion started: 10 December 2019

Streets, D. G., Yarber, K. F., Woo, J. H., and Carmichael, G. R.: Biomass burning in Asia: Annual and seasonal estimates and atmospheric emissions, GLOBAL BIOGEOCHEM CY, 17, n/a-n/a, 10.1029/2003gb002040, 2003.

Stull, R. B.: An introduction to boundary layer meteorology, Atmospheric Sciences Library, 8, Kluwer Academic Publisher, 89 pp., 1988.

Thompson, A. M.: Biomass burning and the atmosphere—accomplishments and research opportunities, ATMOS ENVIRON, 30, i-ii, 10.1016/s1352-2310(96)90021-7, 1996.

Trigg, S., and Flasse, S.: Characterizing the spectral-temporal response of burned savannah usingin situspectroradiometry and infrared thermometry, INT J REMOTE SENS, 21, 3161-3168, 10.1080/01431160050145045, 2000.

Tsuyuzaki, S., Kushida, K., and Kodama, Y.: Recovery of surface albedo and plant cover after wildfire in a Picea mariana forest in interior Alaska, CLIMATIC CHANGE, 93, 517-525, 10.1007/s10584-008-9505-y, 2008.

Uhl, C., and Kauffman, J. B.: Deforestation, fire susceptibility, and potential tree responses to fire in the eastern amazon, Ecology, 71, 437-449, 10.2307/1940299, 1990.

Van Der Werf, G. R., Randerson, J. T., Giglio, L., Collatz, G. J., Kasibhatla, P. S., and Arellano, A. F.: Interannual variability in global biomass burning emissions from 1997 to 2004, ATMOS CHEM PHYS, 6, 3423-3441, 10.5194/acp-6-3423-2006, 2006.

Van Der Werf, G. R., Randerson, J. T., Giglio, L., Collatz, G. J., Mu, M., Kasibhatla, P. S., Morton, D. C., Defries, R. S., Jin, Y., and Van Leeuwen, T. T.: Global fire emissions and the contribution of deforestation, savanna, forest, agricultural, and peat fires (1997–2009), ATMOS CHEM PHYS, 10, 11707-11735, 10.5194/acp-10-11707-2010, 2010.

Veraverbeke, S., Verstraeten, W. W., Lhermitte, S., Van De Kerchove, R., and Goossens, R.: Assessment of post-fire changes in land surface temperature and surface albedo, and their relation with fire - burn severity using multitemporal MODIS imagery, INT J WILDLAND FIRE, 21, 243, 10.1071/wf10075, 2012.

Wallace, J. M., and Hobbs, P. V.: Atmospheric Science (Second Edition), Academic Press, 2006.

Wang, J. D., Wang, S. X., Voorhees, A. S., Zhao, B., Jang, C., Jiang, J. K., Fu, J. S., Ding, D., Zhu, Y., and Hao, J. M.: Assessment of short-term PM2.5-related mortality due to different emission sources in the Yangtze River Delta, China, ATMOS ENVIRON, 123, 440-448, 10.1016/j.atmosenv.2015.05.060, 2015.

Wang, J. D., Xing, J., Mathur, R., Pleim, J. E., Wang, S., Hogrefe, C., Gan, C. M., Wong, D. C., and Hao, J.: Historical Trends in PM2.5-Related Premature Mortality during 1990-2010 across the Northern Hemisphere, ENVIRON HEALTH PERSP, 125, 400-408, 10.1289/EHP298, 2017.

Wang, Z. L., Huang, X., and Ding, A. J.: Dome effect of black carbon and its key influencing factors：a one-dimensional modelling study, 10.5194/acp-18-2821-2018, 2018.

Wiedinmyer, C., Akagi, S. K., Yokelson, R. J., Emmons, L. K., Al-Saadi, J. A., Orlando, J. J., and Soja, A. J.: The Fire INventory from NCAR (FINN): a high resolution global model to estimate the emissions from open burning, 4, 625-641, 10.5194/gmd-4-625-2011, 2011.

Xie, Y. N., Ding, A. J., Nie, W., Mao, H. T., Qi, X. M., Huang, X., Xu, Z., Kerminen, V. M., Petäjä, T., Chi, X. G., Virkkula, A., Boy, M., Xue, L. K., Guo, J., Sun, J. N., Yang, X. Q., Kulmala, M., and Fu, C. B.: Enhanced sulfate formation by nitrogen dioxide: Implications from in situ observations at the SORPES station, J GEOPHYS RES-ATMOS, 120, 12679-12694, 10.1002/2015jd023607, 2015.

Xu, Z. N., Huang, X., Nie, W., Shen, Y. C., Zheng, L. F., Xie, Y. N., Wang, T. Y., Ding, K., Liu, L. X., Zhou, D. R., Qi, X. M., and Ding, A. J.: Impact of Biomass Burning and Vertical Mixing of Residual-Layer Aged Plumes on Ozone in the Yangtze River Delta, China: A Tethered-Balloon Measurement and Modeling Study of a Multiday Ozone Episode, J GEOPHYS RES-ATMOS, 123, 11,786-711,803, 10.1029/2018jd028994, 2018.

https://doi.org/10.5194/acp-2019-957
Preprint. Discussion started: 10 December 2019

Yang, Y. J., Fu, Y. F., Wu, B. W., Shi, C. E., Deng, X. L., Zhang, H., and Zhang, Y.: Impacts of Agricultural Fire on Aerosol Distribution over East China During Summer Harvest Time, Journal of Atmospheric and environmenal optics, 10.3969/j.issn.1673—6141.2013.04.001, 2013.

Yang, Y. J., Yim, S. H. L., Haywood, J., Osborne, M., Chan, J. C. S., Zeng, Z. L., and Cheng, J. C. H.: Characteristics of Heavy Particulate Matter Pollution Events Over Hong Kong and Their Relationships With Vertical Wind Profiles Using High-Time-Resolution Doppler Lidar Measurements, J GEOPHYS RES-ATMOS, DOI: 10.1029/2019JD031140, 2019.

Yin, L. F., Du, P., Zhang, M., Liu, M. X., Xu, T. T., and Song, Y.: Estimation of emissions from biomass burning in China (2003–2017) based on MODIS fire radiative energy data, BIOGEOSCIENCES, 16, 1629-1640, 10.5194/bg-16-1629-2019, 2019.

Zhang, Y., Ding, A. J., Mao, H. T., Nie, W., Zhou, D. R., Liu, L. X., Huang, X., and Fu, C. B.: Impact of synoptic weather patterns and inter-decadal climate variability on air quality in the North China Plain during 1980–2013, ATMOS ENVIRON, 124, 119-128, 10.1016/j.atmosenv.2015.05.063, 2016.

Zhou, D. R., Ding, K., Huang, X., Liu, L. X., Liu, Q., Xu, Z. N., Jiang, F., Fu, C. B., and Ding, A. J.: Transport, mixing and feedback of dust, biomass burning and anthropogenic pollutants in eastern Asia: a case study, ATMOS CHEM PHYS, 18, 16345-16361, 10.5194/acp-18-16345-2018, 2018.

https://doi.org/10.5194/acp-2019-957
Preprint. Discussion started: 10 December 2019

Atmospheric Chemistry and Physics Discussions

Table 1. WRF-Chem domain setting and configuration selections.

Domain setting	
Horizontal grids	130 × 130
Grid spacing	20km × 20km
Vertical layers	30
Map projection	Lambert Conformal
Configuration selections	
Land surface	Noah
Boundary layer	MYJ
Microphysics	Lin et al.
Cumulus	Grell-Freitas
Radiation	CAM
Chemistry	CBMZ
Aerosol	MOSAIC

490

https://doi.org/10.5194/acp-2019-957
Preprint. Discussion started: 10 December 2019

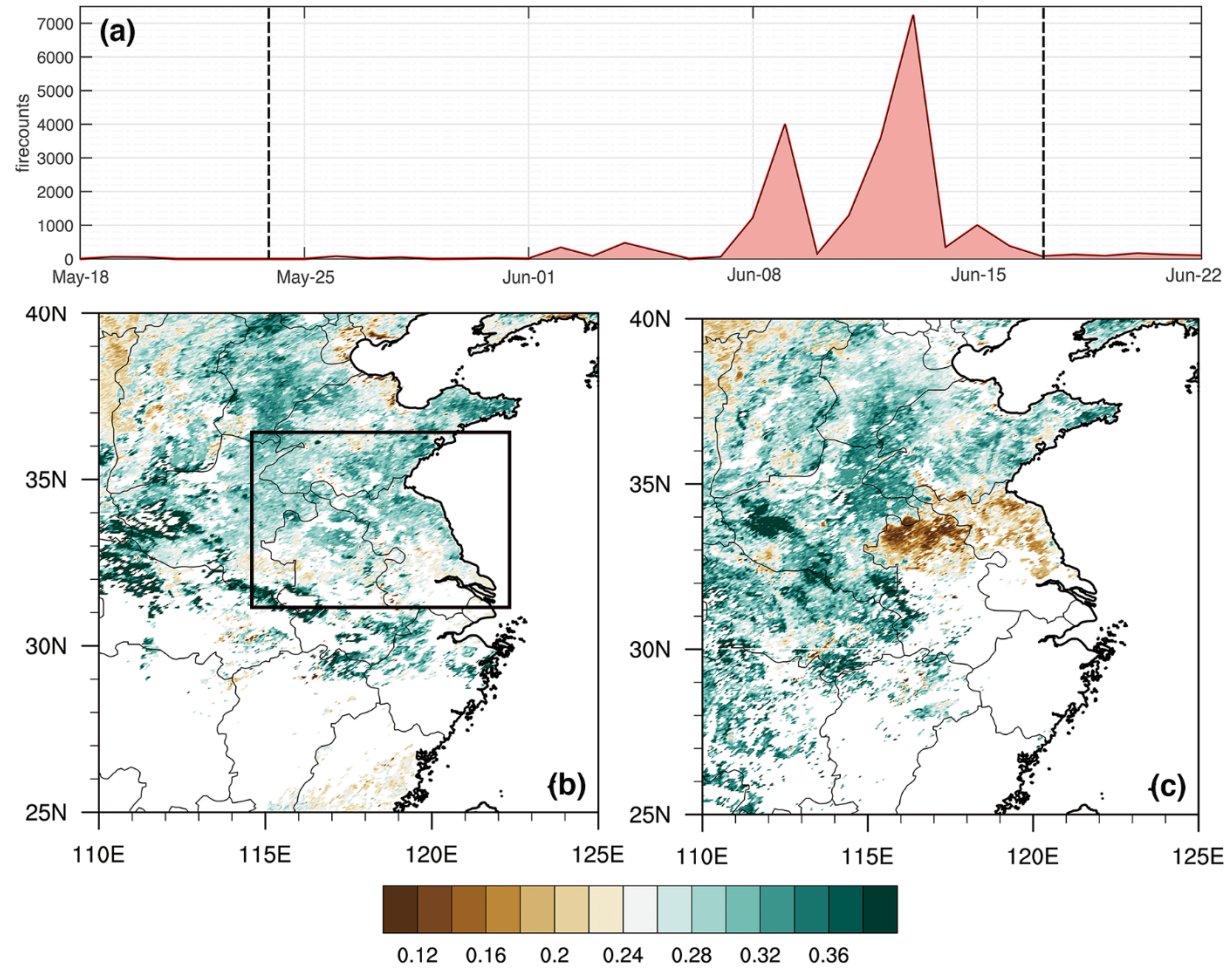

Figure 1. (a) Daily fire counts by MOD/MYD14A1 in the black-boxed zone marked in Fig. 1b and distribution of surface albedo of MODIS Narrow-band2 by MOD09A1 in the northern part of Anhui and Jiangsu Province **(b)** on 24 May, **(c)** on 17 June in 2012 (date marked by black dashed lines in Fig. 1a.)

https://doi.org/10.5194/acp-2019-957
Preprint. Discussion started: 10 December 2019

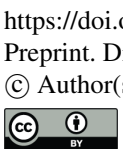

Atmospheric Chemistry and Physics Discussions

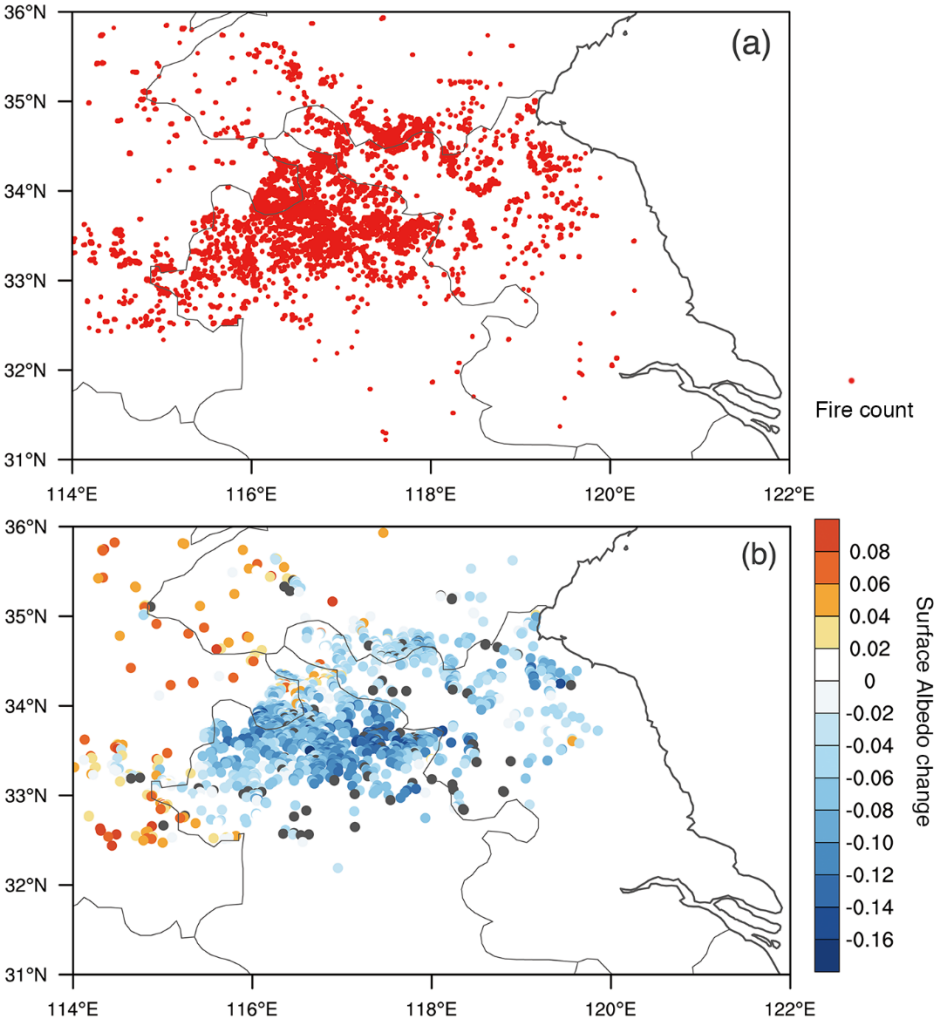

Figure 2. (a) Distribution of high-confidence fire counts by MOD/MYD14A1 accumulated from 24 May to 17 June in 2012, **(b)** Surface albedo change (values on 17 June minus those on 24 May) in the same period by MOD09A1 over corresponding burned area in Fig. 2a. Note: A certain uniform data interval was adopted considering the dots' density.

https://doi.org/10.5194/acp-2019-957
Preprint. Discussion started: 10 December 2019

Atmospheric Chemistry and Physics Discussions

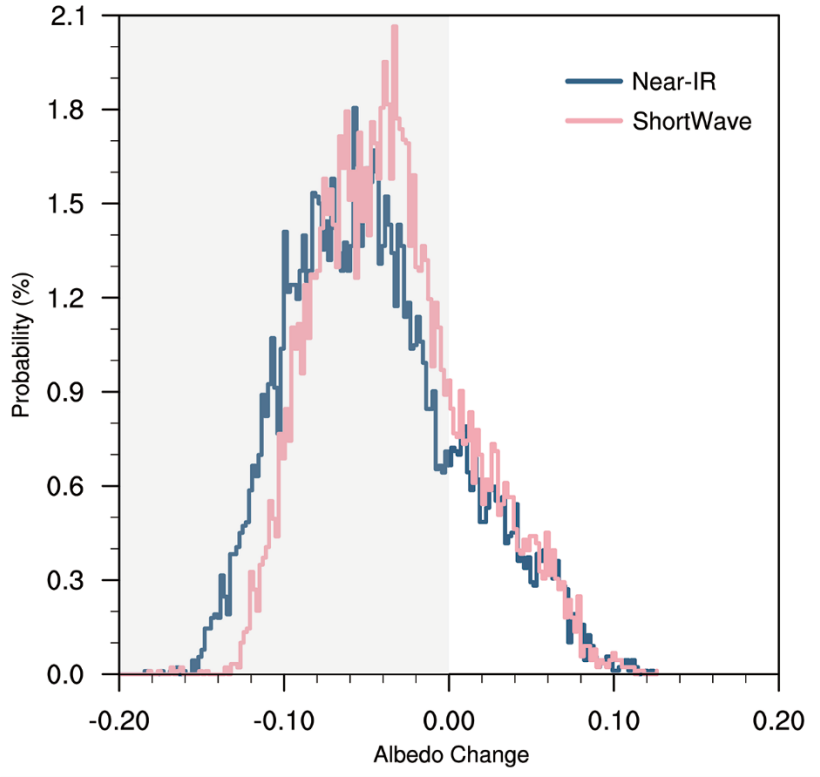

500

Figure 3. Frequency distribution of surface albedo change between 17 June and 24 May by MOD09A1 in fire-count pixels with high confidence by MOD/MYD14A1.

https://doi.org/10.5194/acp-2019-957
Preprint. Discussion started: 10 December 2019

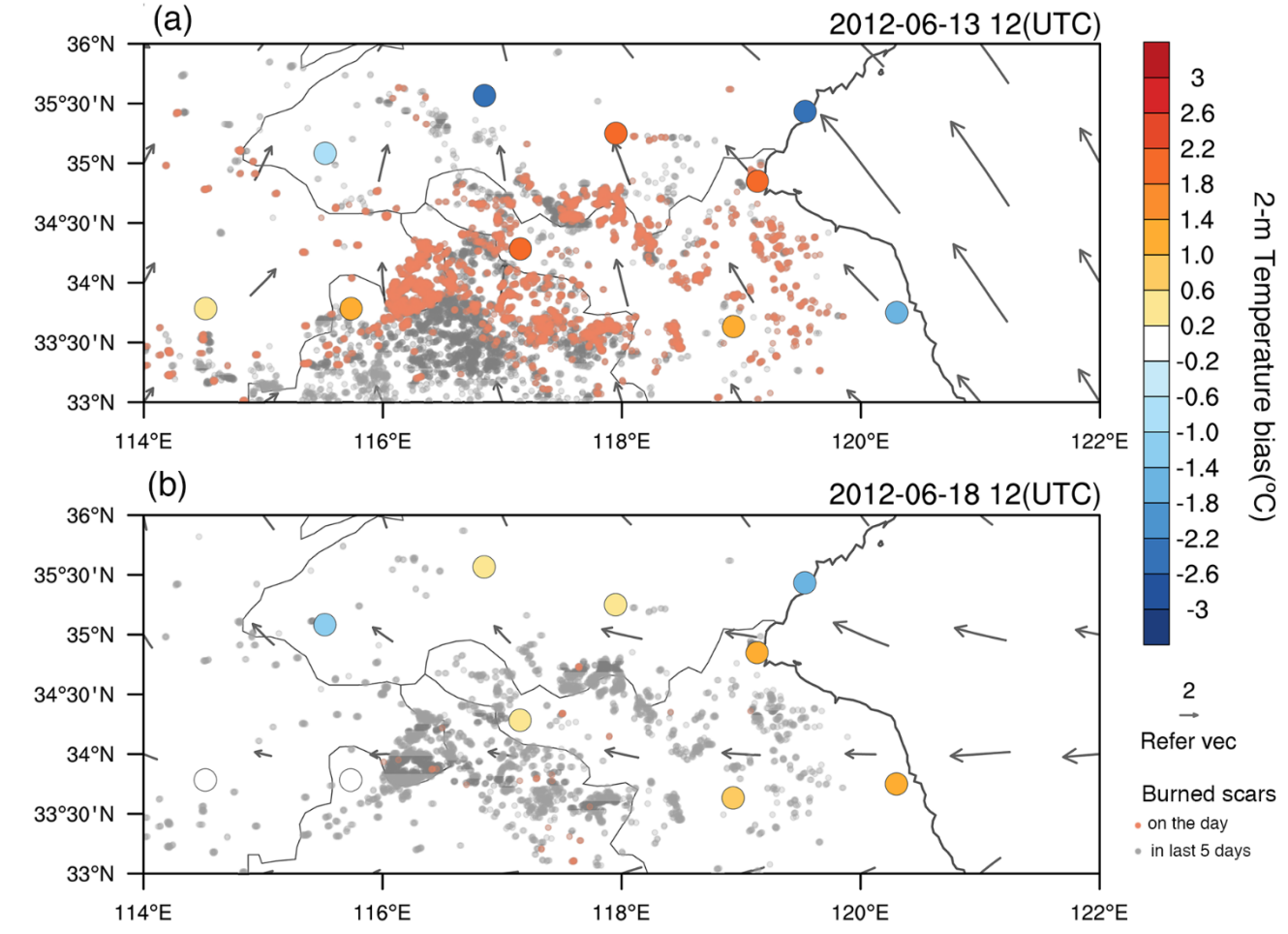

Figure 4. Temperature bias at 2 m height (fill-coloured circles) between FNL analysis data and station observations (OBS) in zone YHR **(a)** on 13 June 2012 and **(b)** on 18 June 2012, at local time 20:00. Bias is defined as value of OBS minus FNL. In Fig. 4a and 4b, grey arrows mark the FNL wind arrow at 10 m height, and grey dots mark the 'burned scar' (defined as accumulated fire counts in the past 5 days) while orange dots mark fire counts on the day.

https://doi.org/10.5194/acp-2019-957
Preprint. Discussion started: 10 December 2019

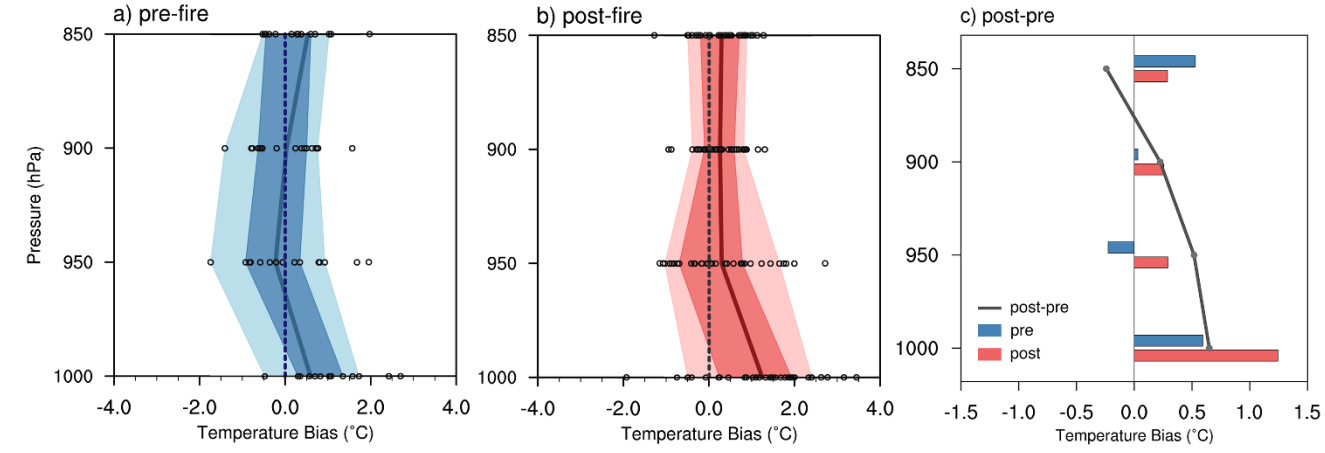

Figure 5. Temperature Bias on isobaric levels between FNL analysis data and sounding observations (OBS) at local time 20:00 at Xuzhou station (marked in Fig. 4a by black box) on clear-sky days before and after BB in June 2007-2015: **(a)** pre-fire **(b)** post-fire. Black circles mark original value of temperature bias (OBS-FNL), dash line marks zero, and the five curves of filled part are respectively 10, 25, 75, 90 percentile and average line in proper order. Bars in **(c)** are the mean value at separate levels and the curve is the corresponding bias between 'post-fire' and 'pre-fire'.

https://doi.org/10.5194/acp-2019-957
Preprint. Discussion started: 10 December 2019

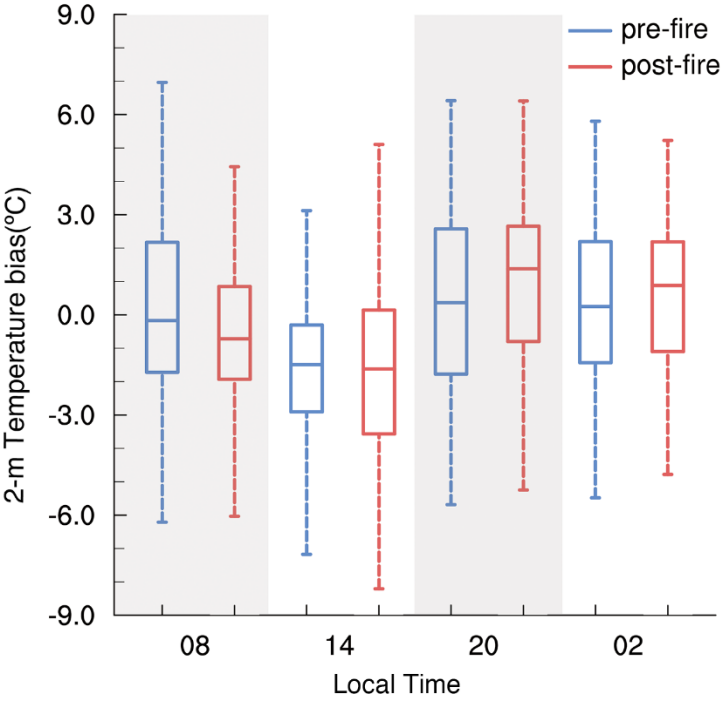

Figure 6. 2-m temperature bias, defined as the value of OBS minus FNL, at stations over fire prone area at local time 08:00, 14:00, 20:00, 02:00 under clear-sky condition pre/post fire in 2007-2015.

520

https://doi.org/10.5194/acp-2019-957
Preprint. Discussion started: 10 December 2019

Atmospheric Chemistry and Physics Discussions

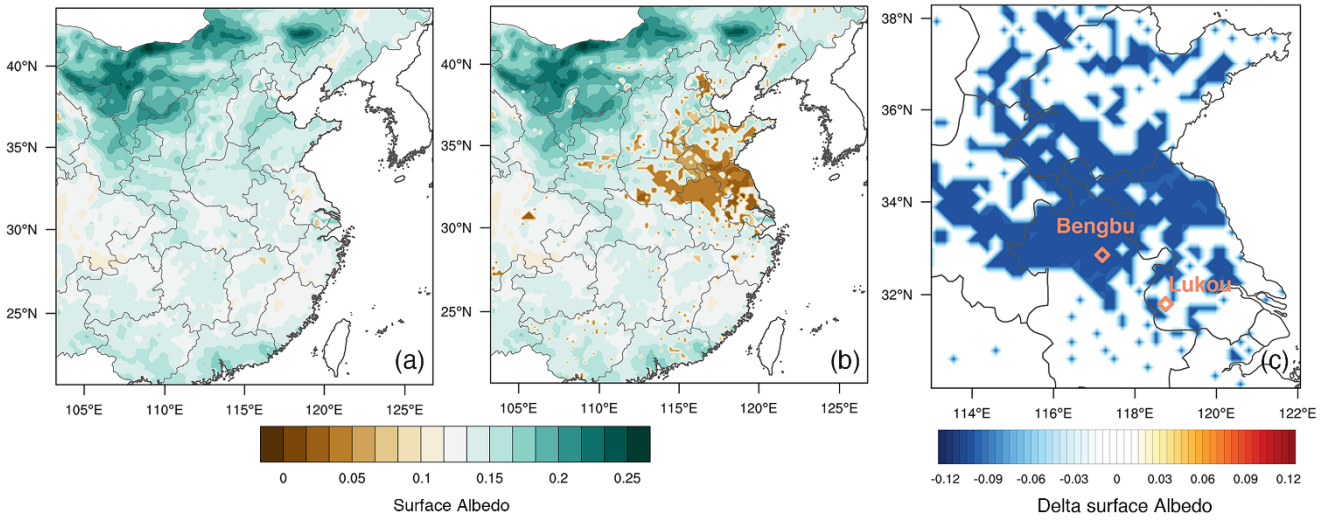

Figure 7. Surface albedo distribution in experiments: (a) CTL and (b) ABD, and (c) difference between the parallel ones (ABD-CTL). Note: Region in Fig. 7c is the enlarged area of the black box in Fig. 7b.

525

https://doi.org/10.5194/acp-2019-957
Preprint. Discussion started: 10 December 2019

Atmospheric Chemistry and Physics Discussions

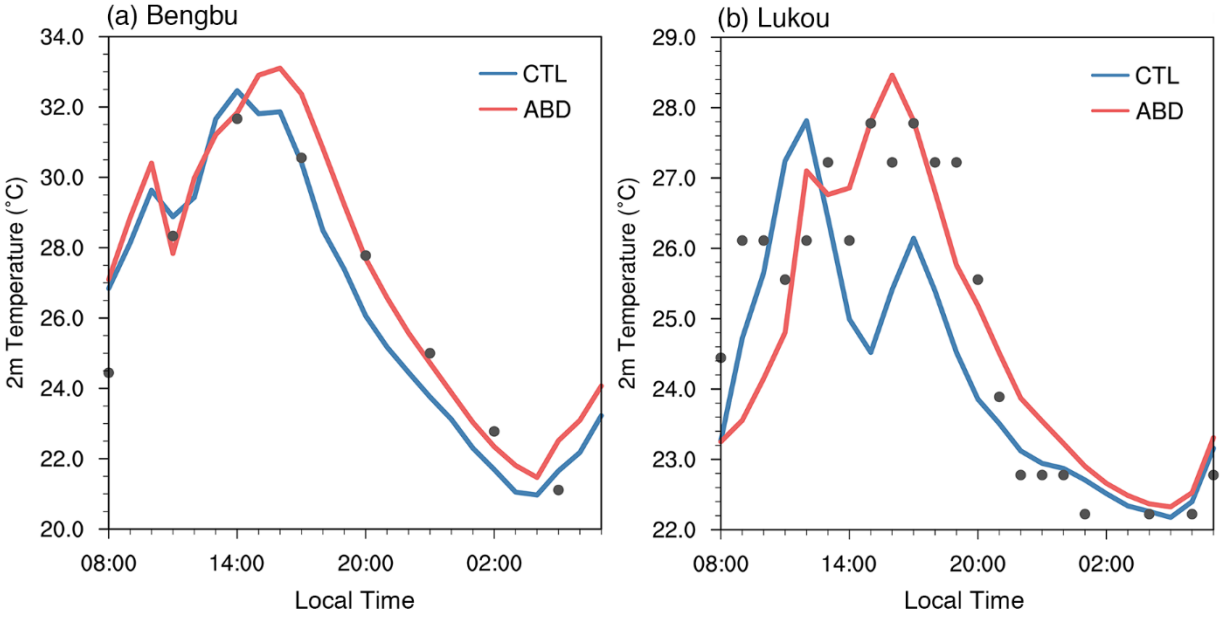

Figure 8. Simulated and observed 2-m temperature at meteorological stations: (a) Bengbu (b) Lukou, on 18 June 2012. Note: Locations of Bengbu and Lukou are marked in Fig. 7c.

530

https://doi.org/10.5194/acp-2019-957
Preprint. Discussion started: 10 December 2019

Atmospheric Chemistry and Physics Discussions

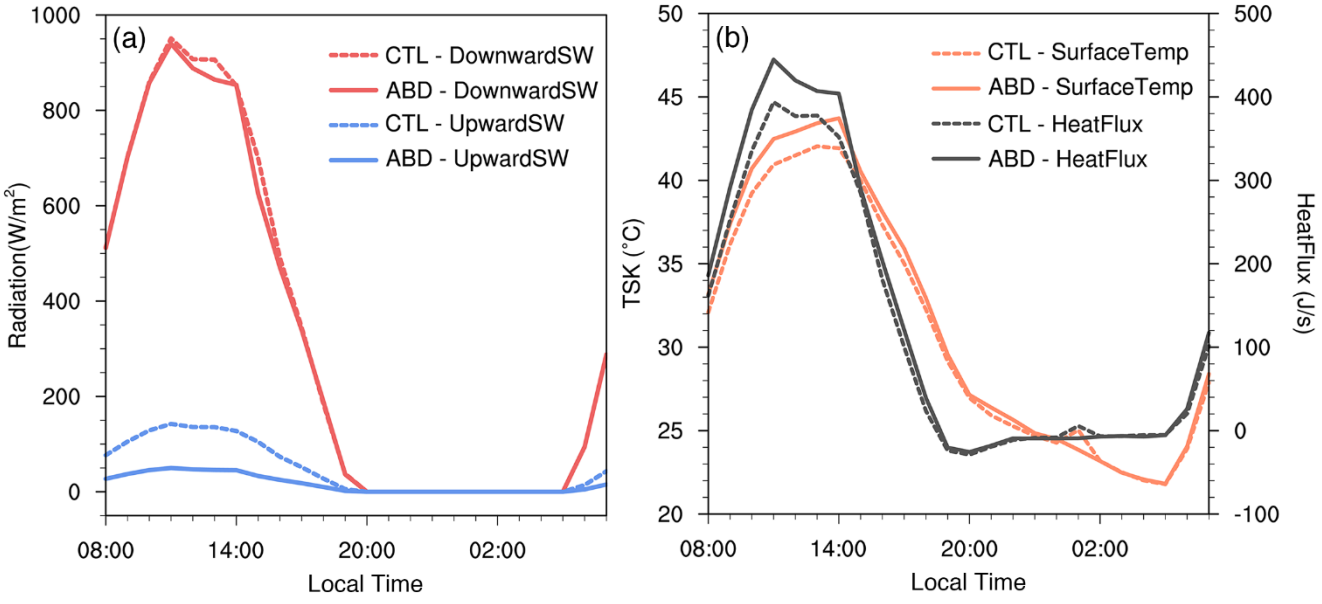

Figure 9. Thermal physical quantities at surface level on 18 June 2012 in experiments CTL and ABD. (a) Down-ward and upward shortwave radiation, (b) Surface temperature and upward heat flux.

https://doi.org/10.5194/acp-2019-957
Preprint. Discussion started: 10 December 2019

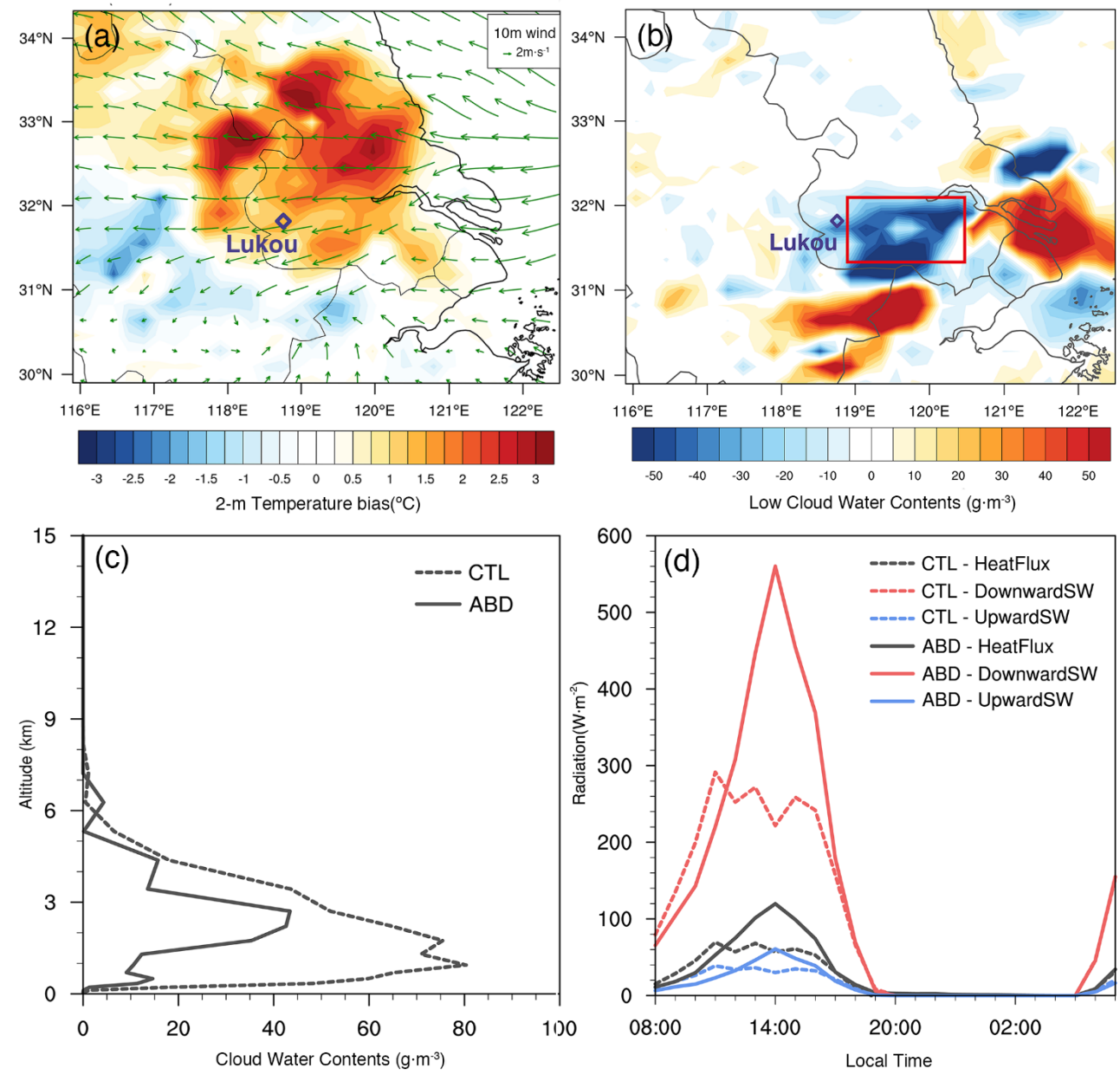

Figure 10. (a) Average 10m-wind in ABD and difference in 2m-temperature between ABD and CTL (ABD-CTL) during the afternoon on 18 June. (b) Average difference in low cloud water content between ABD and CTL (ABD-CTL). (c)Vertical profile of cloud water content during afternoon (d) shortwave radiation and upward heat flux on 18 June averaged in region marked by red rectangle in Fig. 10b.